FEMTOSCOPIC BOSE–EINSTEIN CORRELATIONS OF CHARGED HADRONS IN pp COLLISIONS AT 13 TeV IN CMS* **

Sandra S. Padula

for the CMS Collaboration

Universidade Estadual Paulista (UNESP), São Paulo, SP, Brazil

Femtoscopic correlations between charged hadrons are measured for minimum-bias and for high-multiplicity events in proton–proton collisions at $\sqrt{s} = 13$ TeV. The results are based on data collected with the CMS experiment at the LHC in 2015. Three analysis techniques are employed with different degrees of dependence on simulated events, all of them returning consistent results within the experimental uncertainties. The measured values of the lengths of homogeneity are compared with those from lower energies and from another experiment, and are also discussed in comparison with theoretical predictions.

Two-particle Bose–Einstein correlations (BEC) is a powerful technique for unveiling the size and shape of the source emitting region produced in high-energy collisions. In the Compact Muon Solenoid (CMS) experiment, BEC were studied in Refs. [1, 2] in terms of the invariant pair relative momentum $q_{\mathrm{inv}} = \sqrt{-(k_1 - k_2)^2}$ (k_i^μ is the momentum of each particle of the pair), and in Ref. [3], also in terms of the components of $\boldsymbol{q}$, for exploring the source extent in different directions. The new results reported here were obtained with data produced in pp collisions at 13 TeV, considering events in a very broad range of charged multiplicity, from a few tracks and up to about 250 tracks. As the analysis was performed for the first time in such a broad multiplicity range at these energies, three methods were employed for verifying the independence of the results on the analysis techniques. The first method is the same as in [1–3], the so-called *double ratios* (DR); the second

---

is a data-driven technique (here called *cluster subtraction* — CS) proposed in Ref. [3], and the third method is called *hybrid cluster subtraction* (HCS), similar to that suggested in Ref. [4].

A complete description of the CMS experiment can be found in Ref. [5]. The tracker is the most important part of the detector for this analysis and measures charged particles within the pseudorapidity range of $|\eta| < 2.4$.

This analysis uses data collected during the LHC Run 2 in 2015, recorded with a special collider configuration providing an average of 0.1 interactions per bunch crossing and, therefore, a very low probability of simultaneous proton–proton (pp) collisions (pileup). The events were selected using both minimum-bias (MB) and high-multiplicity (HM) triggers, with samples corresponding to a total integrated luminosity ($\mathcal{L}$) of 0.35 nb^{-1} and 459 nb^{-1}, respectively (for details, see [6]). Simulated event samples employed in this analysis were generated with Monte Carlo (MC) tunes: PYTHIA6.426 Z2*, and PYTHIA8.208 CUETP8M1 for MB events, Z2* and 4C for events with charged particle multiplicity above 95 (see [6] for details), and EPOS1.99 LHC for systematic studies. A complete description of the event and track selections, as well as the triggers used in this analysis can be found in Ref. [6].

Common to the three experimental techniques employed is the analysis is the construction of the single ratios (see Ref. [6] for details), whose numerator contains the Bose–Einstein signal [1–3]. It is obtained by pairing all the same-charge tracks from the same event originating from the primary vertex, with $|\eta| < 2.4$ and $p_{\mathrm{T}} > 0.2$ GeV. The denominator is the background or reference sample, and is formed by pairing particles (all charge combinations) from mixed events, having η within $-2.4 \leq \eta \leq -0.8$, $-0.8 \leq \eta \leq 0.8$ or $0.8 \leq \eta \leq 2.4$ [2]. The single ratio (SR) is then defined as SR $(q_{\mathrm{inv}}) = (\frac{N_{\mathrm{ref}}}{N_{\mathrm{sig}}})\frac{(\mathrm{d}N_{\mathrm{sig}}/\mathrm{d}q_{\mathrm{inv}})}{(\mathrm{d}N_{\mathrm{ref}}/\mathrm{d}q_{\mathrm{inv}})}$, where N_{sig} and N_{ref} are the appropriate normalizations obtained by summing up the pair distribution for all the events in the signal and in the reference sample, respectively. Histograms are then filled with each of these pair distributions separately, in bins of charged particle multiplicity, $k_{\mathrm{T}} = |\boldsymbol{k}_{\mathrm{T}}| = \frac{1}{2}|\boldsymbol{k_{1}}_{\mathrm{T}} + \boldsymbol{k_{2}}_{\mathrm{T}}|$ (pair average transverse momentum), as well as of the relative momentum of the pair q_{inv}.

For obtaining the BEC parameters in the DR method, a double ratio is formed as $\mathrm{DR}(q_{\mathrm{inv}}) = \mathrm{SR}(q_{\mathrm{inv}})/\mathrm{SR}(q_{\mathrm{inv}})_{\mathrm{MC}}$, where $\mathrm{SR}(q_{\mathrm{inv}})_{\mathrm{MC}}$ is the single ratio computed in the same way as in data but with simulated events generated without BEC. The double-ratio procedure is employed for reducing the sources of bias due to track inefficiency and other detector-related effects, as well as for removing non-Bose–Einstein correlations that may remain in the single ratios due to the mixing procedure.

The CS [3] technique uses only SR from data. Correlation functions for opposite-sign (OS) pairs are used for parameterizing the contamination from resonances and jet fragmentation (called "cluster contribution"), which are

still present in the correlation function. The amplitude of these contributions present for the same-sign (SS) pairs is then evaluated by using the same shape as found for OS pairs, while varying the overall scale to fit the data (see Ref. [3] for details). To find the fit parameters, the correlation function is fit with a function composed of the cluster contribution and the Bose–Einstein component (see Ref. [3] for a complete description).

The Hybrid Cluster Subtraction (HCS) method [6], similar to one proposed for pPb data by the ATLAS experiment [4], also employs SR only, using MC SR to relate the amplitudes and the widths of the fits to OS and SS MC correlation functions, by means of "conversion functions". Next, non-BEC effects are estimated by fitting amplitudes and widths of data OS SR. Then the conversion functions estimated with MC simulations are used for converting the fitted parameters from data OS SR into those for data SS SR. Finally, the data SS SR is fitted with a combined function for signal plus cluster contribution altogether.

In the case of charged hadrons, the Coulomb final-state interactions unavoidably contaminate the signal sample. For point-like sources (and for the systems produced in pp collisions), they can be corrected (pairwise, in this analysis) by the Gamow factor which, in the case of the same charge and opposite charge pairs, respectively, is given by $G_w^{\mathrm{SS}}(\eta_w) = |\Psi^{\mathrm{SS}}(0)|^2 = \frac{2\pi\eta_w}{\exp{(2\pi\eta_w)} - 1}$, $G_w^{\mathrm{OS}}(\eta_w) = |\Psi^{\mathrm{OS}}(0)|^2 = \frac{2\pi\eta_w}{1 - \exp{(-2\pi\eta_w)}}$, where $\eta_w = \frac{\alpha_{em}m_\pi}{q_{\mathrm{inv}}}$, α is the fine-structure constant, and m is the particle mass.

The measurements are performed in the local co-moving system (LCMS), where the longitudinal component of the pair average momentum vanishes $(k_{\mathrm{L}} = \frac{1}{2}(k_{1\mathrm{L}} + k_{2\mathrm{L}}) = 0)$. The parameterizations used to fit the BEC functions in one dimension in terms of q_{inv} [1–3, 6] can be written as

$$C_{\mathrm{BE}}(q_{\mathrm{inv}}) = C[1 + \lambda \exp{\{-(q_{\mathrm{inv}} R_{\mathrm{inv}})^a\}}] \, (1 + \epsilon \, q_{\mathrm{inv}}), \qquad (1)$$

where C is a constant, R_{inv} is the (BEC) radius fit parameter, also called the length of homogeneity, and λ is the intercept parameter, corresponding to the intensity of the correlation function at $q_{\mathrm{inv}} = 0$; the additional polynomial term proportional to ϵ describes possible long-range correlations. The exponent a is the Lévy index of stability satisfying the inequality $0 < a \leq 2$ ($a = 1$ characterizes an exponential function and $a = 2$, a Gaussian distribution). In particular, the case $a = 1$ employed in this analysis, the exponential terms in Eq. (1) coincide with the Fourier transform of the source function $\rho(t, \boldsymbol{x})$ describing a Lorentzian or Cauchy distribution.

Several sources of systematic uncertainties were investigated, the largest being from the reference samples and from the MC tunes, in all three methods. Within the HCS method, the overall values integrated in k_{T} correspond to variations of 5–20% in R_{inv} (and λ) in different multiplicity ranges.

Results for the lengths of homogeneity obtained with each of the three methods are presented in Fig. 1. The left plot shows R_{inv} as a function of the average multiplicity $\langle N_{\mathrm{tracks}} \rangle$, for values of k_{T} integrated in the range of $0 < k_{\mathrm{T}} < 1$ GeV. The radius fit parameter increases as a function of multiplicity, showing a change of slope around $\langle N_{\mathrm{tracks}} \rangle \sim 20$–$30$ and a tendency to saturate at higher multiplicities. The right plot shows R_{inv} obtained in two multiplicity bins, MB ($N_{\mathrm{track}}^{\mathrm{offline}} < 80$) and HM ($N_{\mathrm{track}}^{\mathrm{offline}} > 80$), as a function of k_{T}. The lengths of homogeneity tend to decrease for increasing k_{T}, more so at lower multiplicity. This behavior is compatible with an emitting source that was expanding prior to decoupling. The three methods return compatible results within the experimental uncertainties, even in the most conservative case, where they were assumed to be fully correlated. Therefore, when comparing to other energies and to theoretical models, only the values found using the HCS method are shown, chosen for being less sensitive to MC tunes than in the DR method, and for having smaller systematic uncertainties than in the CS method. The ratio of RMS over mean for the differences between R_{inv} values in each of the three methods is adopted as a relative uncertainties due to the variations between techniques.
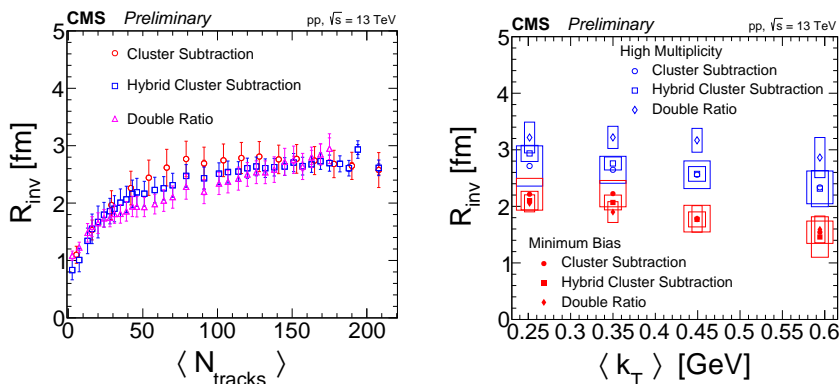

Fig. 1. Results for R_{inv} in the three methods are shown as a function of $\langle N_{\mathrm{tracks}} \rangle$ (left) and k_{T} (right). For enhancing visibility, statistical and systematical uncertainties are represented either by internal and external error bars, respectively (left), or, as allowed in the case of wider bins, by error bars and by open boxes with variable widths for each of the three methods, respectively (right) [6].

The lengths of homogeneity for pp collisions at 13 TeV are compared in Fig. 2, as a function of multiplicity, with the corresponding results obtained in pp collisions at 7 TeV by CMS [3] (left) and ATLAS [7] (right), showing good agreement in both cases.

The Color Glass Condensate (CGC) calculations [8] predict an increase of the interaction radius (resulting from the initial overlapping of the two protons) for charged particles per unit rapidity above 5 and up to $(\mathrm{d}N/\mathrm{d}y)^{1/3} \sim$
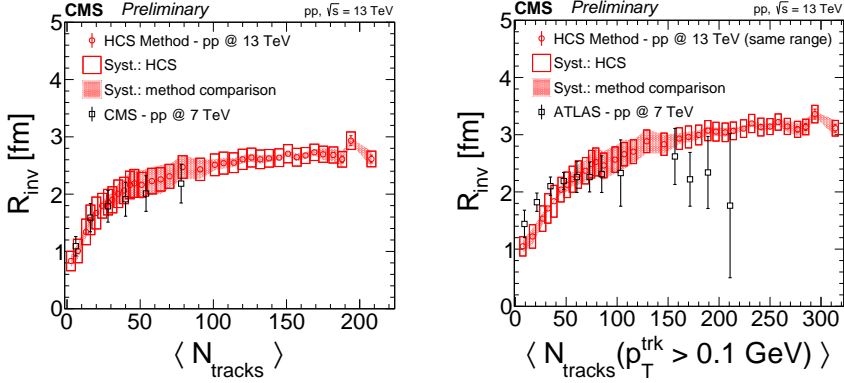
Fig. 2. Lengths of homogeneity as a function of charged particle multiplicity obtained with the HCS method in *pp* collisions at 13 TeV [6] are compared with corresponding results obtained in *pp* collisions at 7 TeV from CMS (left) and ATLAS (right).

3.4 [8]. Beyond this point, the radius tends to a constant value, the so-called "saturation" radius. The parameterization in Ref. [8] (see Ref. [6] for details) is compared with results from the HCS method in Fig. 3 (left). The predictions from the CGC for the saturation radius are clearly below the trend shown in the data. This underestimate may be due to considering only the initial *pp* size and energy density in the calculations, without adding any fluid dynamic evolution prior to emission [9]. If the same parametrization as in [8] is used, but treating the coefficients as free parameters, the results in Fig. 3 (left) are in good agreement with the data.
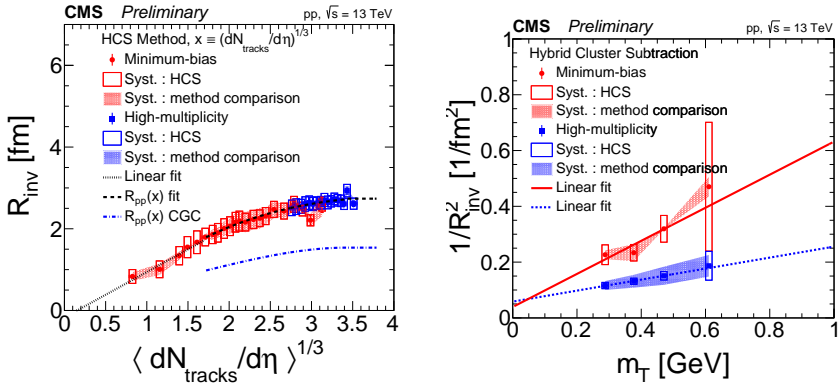

Fig. 3. Left: Radius from the HCS method as compared to the predictions from the CGC as a function of $(\langle N_{\text{tracks}} \rangle / \mathrm{d}\eta)^{1/3}$. Right: $1/R_{\text{inv}}^2$ as a function of $m_{\text{T}} = \sqrt{m_\pi^2 + \langle k_{\text{T}} \rangle^2}$ for the HCS method. Only statistical uncertainties are considered in all fits (see details in Ref. [6]).

Theoretical predictions based on hydrodynamical models are not yet available for pp collisions at 13 TeV. However, expectations for qualitative trends can be found in the literature [10, 11], showing that the three components of the radius fit parameters continuously grow with $\langle N_{\text{tracks}} \rangle^{1/3}$ for pp collisions. This behavior is in qualitative agreement with the left plot of Fig. 3 and was also observed in different collision systems (CuCu, AuAu, PbPb, and pp) and energies (ranging from 62.4 GeV to 7 TeV) (see Ref. [10]). In addition, hydrodynamic models can provide valuable information about the collective transverse expansion of the system (transverse flow) by studying the behavior of $1/R_{\text{inv}}^2$ *versus* $m_{\text{T}} = \sqrt{m_\pi^2 + \langle k_{\text{T}} \rangle^2}$ (m_π is the pion mass) by means of the slope of the associated linear fit. Furthermore, the value of $1/R_{\text{inv}}^2$ at $m_{\text{T}} = 0$ can unveil the final-state geometrical size of the source, which is significant information to complement the BEC investigation conducted in this analysis (see Ref. [6] and references therein). This is shown in the right plot of Fig. 3, where the expansion in the MB region happens at a higher rate than in the HM region. From this plot, the corresponding geometrical size can be extracted for the MB and the HM regions, resulting in $R_{\text{G}}^{\text{MB}} = 5.1 \pm 0.4$ fm and $R_{\text{G}}^{\text{HM}} = 4.2 \pm 1.1$ fm, respectively.

The proportionality of $R^{-2} \propto a + b\, m_{\text{T}}$ (which was universally observed in AA collisions for different colliding system sizes, collision energies, and centrality) implies that the lengths of homogeneity are driven by initial geometry, as well as by transverse flow (and also longitudinal flow in a 3D analysis). This observation, also seen in the present case, suggests that such phenomenological modeling also applies to pp collisions at the LHC energies.

REFERENCES

[1] V. Khachatryan *et al.* [CMS Collaboration], *Phys. Rev. Lett.* **105**, 032001 (2010).

[2] V. Khachatryan *et al.* [CMS Collaboration], *J. High Energy Phys.* **1105**, 029 (2011).

[3] A.M. Sirunyan *et al.* [CMS Collaboration], *Phys. Rev. C* **97**, 064912 (2018).

[4] M. Aaboud *et al.* [ATLAS Collaboration], *Phys. Rev. C* **96**, 064908 (2017).

[5] S. Chatrchyan *et al.* [CMS Collaboration], *JINST* **3**, S08004 (2008).

[6] The CMS Collaboration, Physics Analysis Summary CMS-PAS-FSQ-15-009, 2018, `https://cds.cern.ch/record/2318575`

[7] G. Aad *et al.* [ATLAS Collaboration], *Eur. Phys. J. C* **75**, 466 (2015).

[8] L. McLerran, M. Praszalowicz, B. Schenke, *Nucl. Phys. A* **916**, 210 (2013).

[9] A. Bzdak *et al.*, *Phys. Rev. C* **87**, 064906 (2013).

[10] P. Bożek, W. Broniowski, *Phys. Lett. B* **720**, 250 (2013).

[11] V.M. Shapoval *et al.*, *Phys. Lett. B* **725**, 139 (2013).